

# Germline PTPRT mutation potentially involved in cancer predisposition

Lorena Martín<sup>1</sup>, Victor Lorca<sup>2</sup>, Pedro Pérez-Segura<sup>2</sup>, Patricia Llovet<sup>1</sup>, Vanesa García-Barberán<sup>3</sup>, Maria Luisa Gonzalez-Morales<sup>2</sup>, Sami Belhad<sup>4</sup>, Gabriel Capellá<sup>5</sup>, Laura Valle<sup>4</sup>, Miguel de la Hoya<sup>2</sup>, Pilar Garre<sup>6</sup>, and Trinidad Caldes<sup>2</sup>

<sup>1</sup>Hospital Clinico San Carlos. IdISCC

<sup>2</sup>Hospital Clinico San Carlos. IdISSC

<sup>3</sup>Hospital Clínico San Carlos, IdISCC, CIBERONC

<sup>4</sup>IDIBELL

<sup>5</sup>ICO-IDIBELL

<sup>6</sup>Hospital clinico San Carlos. IdISSC

September 17, 2020

## Abstract

Familial Colorectal Cancer Type X (FCCTX) is a term used to describe a group of families with an increased predisposition to colorectal and other related cancers, but an unknown genetic basis. Whole-exome sequencing in two cancer-affected and one healthy members of a FCCTX family revealed a truncating germline mutation in PTPRT [c.4090dup, p.(Asp1364GlyfsTer24)]. PTPRT encodes a receptor phosphatase and is a tumor suppressor gene found to be frequently mutated at somatic level in many cancers, having been proven that these mutations act as drivers that promote tumor development. This germline variant shows a compatible cosegregation with cancer in the family and results in the loss of a significant fraction of the second phosphatase domain of the protein, which is essential for PTPRT's activity. In addition, the tumors of the carriers exhibit epigenetic inactivation of the wild-type allele and an altered expression of PTPRT downstream target genes, consistent with a causal role of this germline mutation in the cancer predisposition of the family. Although PTPRT's role cancer initiation and progression has been well studied, this is the first time that a germline PTPRT mutation is linked with cancer susceptibility and hereditary cancer, which highlights the relevance of the present study.

## Introduction

Hereditary Non-Polyposis Colorectal Cancer (HNPCC) is an autosomal dominant inherited condition characterized by an increased susceptibility to colorectal cancer (CRC) and other associated tumors and defined by the Amsterdam I and II clinical criteria (Vasen, Mecklin, Khan, & Lynch, 1991; Vasen, Watson, Mecklin, & Lynch, 1999). An important fraction of these families is known as Lynch Syndrome and is caused by germline inactivating mutations in the mismatch repair (MMR) genes, which results in microsatellite instability (MSI) in the tumors. However, it is estimated that almost half of the families that fulfill the Amsterdam criteria do not present any defects in the MMR genes. For this reason, the term Familial Colorectal Cancer Type X (FCCTX) emerged to designate such group of HNPCC families with microsatellite stable, MMR-proficient tumors, for whom the genetic basis underlying their predisposition to CRC and other related cancers remains to be elucidated (Lindor, 2009). Although the arrival of Next Generation Sequencing (NGS) has allowed the identification of new CRC predisposition genes (Esteban-Jurado et al., 2016; Evans, Green, & Woods, 2018; Garre et al., 2011, 2015; Martín-Morales et al., 2017; Nieminen et al., 2014; Schulz et al., 2014; Seguí et al., 2015; Smith et al., 2013; Valle, 2017), most FCCTX cases remain unexplained. In fact, FCCTX comprises

a heterogeneous group of families that presumably includes different genetic syndromes involving high or moderate-penetrance mutations in novel cancer-predisposing genes, but that could also result from a combination of low-penetrance mutations in different genes (Zetner & Bisgaard, 2017). Therefore, identifying the genetic cause of the increased cancer susceptibility in FCCTX families is still a challenge.

- 1.
- 2.

Tyrosine phosphorylation is a covalent post-transcriptional modification that is essential for signal transduction, regulating many processes in all eukaryotic cells (Hunter, 2009). Thus, perturbations in tyrosine phosphorylation are involved in many human diseases (Singh et al., 2017). Given that this modification is coordinately regulated by protein tyrosine kinases (PTKs) and protein tyrosine phosphatases (PTPs), genetic and epigenetic alterations in genes encoding PTKs and PTPs can result in changes to the equilibrium of kinase-phosphatase activity that might have a deleterious effect and produce abnormal cell proliferation, which could ultimately lead to cancer (Julien, Dubé, Hardy, & Tremblay, 2011). In fact, many PTKs have been long known to act as oncogenes in cancer initiation and progression, while most PTPs have been proven to act as tumor suppressors, reversing the negative effects of PTKs (Julien et al., 2011).

Wang et al. (Z. Wang et al., 2004) were the first to discover that PTPs are frequently mutated in CRC, and it was later discovered that PTPs are somatically mutated in many other cancers, playing particularly important roles in colon and endometrium cancers (S. Zhao, Sedwick, & Wang, 2015). Among all PTP genes, *PTPRT* is the most frequently mutated in human cancers, with somatic mutations identified in 11% of colon, 11% of esophagus, 10% of lung, 9% of stomach, 8% of endometrium, 6% of bladder and 6% of head and neck cancers, as well as in a smaller fraction of leukemia, breast, ovary, liver, pancreas and prostate tumors (S. Zhao et al., 2015). Noteworthy, these somatic mutations have been proven to act as driver mutations, leading to cancer initiation and progression (L.-E. Wang et al., 2013). Another mechanism leading to the loss of *PTPRT* function is the frequent hypermethylation of its promoter, which has been recently reported in colorectal (Laczmanska et al., 2013) and head and neck tumors (Peyser et al., 2016).

*PTPRT* or *PTP $\rho$*  (Protein Tyrosine Phosphatase Receptor Type T or Rho) belongs to the type IIB subfamily of classical receptor PTPs (class I). Besco et al. showed that *PTPRT* interacts with adherence junction components through its extracellular region and that most tumor-derived mutations located in this domain impair cell-cell adhesion (Besco, Hooft van Huijsduijnen, Frosthalm, & Rotter, 2006). On the other hand, the cytoplasmatic segment of this subfamily consists of a cadherin-like juxtamembrane domain and two phosphatase domains: D1 and D2. It is generally believed that the membrane-proximal PTP domain (D1) is responsible for the tyrosine phosphatase activity per se, whereas the second is a pseudo-phosphatase domain (D2) that has no phosphatase activity (Tonks, 2006). However, many tumor-derived mutations are located in the second catalytic domain (Z. Wang et al., 2004), suggesting that this domain has an important structural function or harbors a still unknown enzymatic activity. As a matter of fact, both catalytic domains have been proven to be essential for the correct function of the protein, and it has been suggested that D2 may be important for the regulation of the phosphatase activity (X. Zhang et al., 2007).

Regarding its substrates, two main proteins have been reported to be modified by *PTPRT*, *STAT3* and *paxillin*, both of which are well-known oncogenes that are inactivated upon dephosphorylation by *PTPRT* (X. Zhang et al., 2007; Y. Zhao et al., 2010) (Supplementary Figure S1). *PTPRT* specifically dephosphorylates *STAT3*'s residue Y705 (X. Zhang et al., 2007), whose phosphorylation is key for *STAT3* activation (Darnell, 2005). It has been shown that pY705 *STAT3* is up-regulated in a variety of human cancers, playing an oncogenic role in tumor development (Darnell, 2005; Lui et al., 2014; P. Zhang et al., 2011). *PTPRT*-dependent inactivation of *STAT3* has been reported to reduce the expression of two of *STAT3* target genes (*Bcl-XL* and *SOCS3*) in CRC cells, proving *PTPRT*'s role as an inhibitor of the IL6-JAK-*STAT3* pathway (X. Zhang et al., 2007). On the other hand, *PTPRT* dephosphorylates *paxillin*'s residue Y88, whose phosphorylation has been also proven to be crucial for colorectal tumorigenesis (Y. Zhao et al., 2017, 2010). *PTPRT*-mediated inactivation of *paxillin* results in the decreased phosphorylation of its substrates (such as p130CAS, SHP2

and Akt), hence inhibiting the PI3K-Akt pathway (Y. Zhao et al., 2017, 2010).

With the aim of identifying the genetic cause underlying FCCTX, whole-exome sequencing was performed in a group of 13 Amsterdam-positive MMR-proficient HNPCC families. The present study describes a truncating germline mutation in the *PTPRT* gene that was identified in one of these families.

## Materials and methods

### Study population

The whole exome was studied in 13 FCCTX families recruited at the Genetic Counseling Unit of Hospital Clínico San Carlos (Madrid, Spain). All of the families fulfilled the Amsterdam I or II clinical criteria for HNPCC (Vasen et al., 1991, 1999) and presented MMR-proficient tumors with neither MSI nor lack of expression of MMR proteins. In addition, none of them carried germline mutations in the MMR genes. Other family members, whether healthy or affected, were also recruited for segregation studies. Formalin-fixed paraffin-embedded (FFPE) tumor blocks from the probands and/or their cancer-affected relatives were obtained whenever available. Information on personal and family cancer history was obtained, and cancer diagnoses were confirmed by medical and pathology records. The study was approved by the Institutional Review Board of Hospital Clínico San Carlos, and a written informed consent was signed by each participant.

An independent series of 473 genetically unexplained MMR-proficient familial and/or early-onset non-polyposis CRC unrelated patients recruited at the Institut Català d'Oncologia (IDIBELL, Barcelona, Spain), was included for validation purposes (Belhadj et al., 2019). While 443 fulfilled the Amsterdam or Bethesda (Umar et al., 2004) criteria at the time of referral to the genetic counseling, 30 did not but were included in the study based on a clinical referral for non-polyposis CRC and absence of MMR deficiency. Healthy individuals with no cancer family history were recruited from the Blood Bank of Hospital Clínico San Carlos (Madrid) and used as controls. FFPE tumor blocks obtained from sporadic CRC patients were used as CRC controls, while FFPE blocks containing non-tumor colon tissue were used as healthy colon controls. All of these control subjects had previously signed an informed consent.

### DNA and RNA extraction and quantification

Germline DNA and RNA were extracted from peripheral blood using the MagNA Pure Compact extractor system (Roche Diagnostics), according to the manufacturer's recommendations. The PAXgene Blood RNA Kit (PreAnalytiX) was used to extract germline RNA when the patient could not come to our hospital. Tumor DNA and RNA were extracted from 7 $\mu$ m-thick FFPE tissue sections, and a hematoxylin and eosin-stained section of each block allowed the assessment of tumor cell area and content by two experienced pathologists. Tumor DNA was purified using the QIAamp DNA FFPE Tissue Kit from Qiagen, while tumor RNA was isolated employing the RNeasy FFPE Kit (Qiagen), according to their corresponding protocols. The NanoDrop ND-1000 Spectrophotometer was used to assess the DNA and RNA quantity and quality. However, for NGS purposes, the quality of DNA samples was also tested by agarose gel electrophoresis and the concentration of the samples was measured in a Qubit 3.0 Fluorometer (Life Technologies) and a 2100 Bioanalyzer (Agilent).

- 1.
- 2.

### Whole-exome sequencing

Whole-exome sequencing was outsourced to Sistemas Genómicos (Valencia, Spain). The exome capture was performed using SureSelectXT Human All Exon V3 (51Mb, Agilent Technologies), and the library was sequenced on an Illumina HiSeq 2000 platform with paired-end reads of 101bp and a 50x average coverage depth. Reads were trimmed and subsequently aligned against the human reference genome version GRCh37/hg19 using the BWA software, followed by processing by Picard-tools and SAMtools. Variant calling was performed using a combination of two different algorithms (VarScan and GATK) and the identified

variants were annotated and described according to the recommendations of the Human Genome Variation Society.

### Variant filtering and prioritization

The variants identified by whole-exome sequencing were subsequently filtered for the selection of those variants that were: 1) shared by the cancer-affected family members sequenced; 2) carried in heterozygosity; 3) coding (frameshift, inframe, nonsense, splicing or missense) and affecting autosomes; 4) rare (minor allele frequency (MAF)  $\geq 0.01$  in the general population) and not present in 3 or more families; 5) predicted to be damaging by least 4 out of 5 *in silico* tools for missense variants and 2 out of 2 for inframe variants, or predicted to alter splicing for splice region variants; and 6) absent in a healthy elderly relative sequenced (when applicable). Finally, the filtered variants were prioritized based on the relevance of the gene and the location of the variant in the protein structure, allowing the selection of a list of candidate variants.

### *In silico* studies

The MAF of the identified variants in the general population was checked in three different databases: 1000 Genomes Project, Exome Variant Server and GnomAD. On the other hand, the *in silico* tools used for the damage prediction were SIFT, PolyPhen, Condel, MutationTaster and PROVEAN for missense variants, and only the last two for inframe variants. This was done with the help of Ensembl's Variant Effect Predictor tool. Splicing alterations were predicted by the Human Splicing Finder. For variant prioritization, all genes affected by filtered variants were thoroughly examined with UniProt, OMIM, Reactome, PathCards, Pubmed, STRING, SMART and cBioPortal's MutationMapper. The 3D structure of the genes affected by these variants was simulated by SWISS-MODEL in order to visualize the effects of the mutations on the protein structure.

### Variant validation, segregation and loss of heterozygosity (LOH) studies

Candidate variants were validated by PCR followed by Sanger sequencing of the corresponding region of each gene. The segregation and LOH studies for the *PTPRT* variant were also assessed by Sanger sequencing of the selected area of the *PTPRT* gene (exon 30, ENST00000373198). The segregation study was carried out in germline DNA from the available members of the family. For the LOH analyses, tumor and germline DNA were assessed by Sanger sequencing and the corresponding electropherograms were compared in order to detect possible variations in the peak height of any of the alleles. All the primers used are described in Supplementary Table S2.

### Promoter methylation assay

The promoter methylation assay consisted of an initial bisulfite conversion of 1 $\mu$ g of DNA using the EpiTect Bisulfite Kit (Qiagen), followed by a methylation specific PCR (MSP) using the EpiTect MSP Kit (Qiagen) and two different sets of specific primers targeting the promoter region of *PTPRT*. Each set was composed of 2 pairs of primers, which specifically detected methylated or unmethylated DNA and had been previously described by Laczmanska et al. (Laczmanska et al., 2013) (in CRC) or by Peyser et al. (Peyser et al., 2016) (in head and neck carcinoma) (Supplementary Table S2). Tumor DNA from two *PTPRT* mutation carriers was used for this assay, while DNA obtained from healthy colon or breast tissue was used as a control. The bisulfite conversion and MSP were carried out following the manufacturers' instructions, and the PCR products were then analyzed by agarose gel electrophoresis.

### Pyrosequencing

A pyrosequencing assay was also used for the measurement of *PTPRT* promoter methylation. For that purpose, the bisulfite conversion of 1 $\mu$ g of DNA using the EpiTect Bisulfite Kit (Qiagen) was followed by a PCR targeting a fraction of *PTPRT* promoter. Finally, the pyrosequencing took place in a PyroMark Q96 MD sequencer (Biotage, Qiagen), taking advantage of the PyroMark Q96 reagents and buffers and following the manufacturer's instructions. Tumor or healthy tissue DNA from *PTPRT* mutation carriers was used for this assay, while commercial high-methylated and non-methylated DNA was used as a control (CpGenome

Human Methylated/Non-Methylated DNA Standard, Millipore). The PCRs and subsequent pyrosequencing were performed in triplicates, and the relative methylation (%) and standard deviation were represented. The sequences of the PCR and biosynthesis primers are shown in Supplementary Table S2.

### Reverse transcription PCR (RT-PCR)

RT-PCR was performed using the PrimeScript RT Reagent Kit (Perfect Real Time, Takara, Clontech), following the kit's instructions. The absence of genomic DNA (gDNA) in cDNA samples was confirmed prior to their use by a PCR targeting exons 2-3 of *PALB2*, which allowed the discrimination between gDNA and cDNA. The primers used for this test are available upon request.

### Digital PCR (dPCR)

For the allele-specific expression assay, a custom TaqMan dPCR was carried out taking advantage of the QuantStudio 3D Digital PCR System (Applied Biosystems) and according to the manufacturer's recommendations. Specific TaqMan probes were designed with the Custom TaqMan Assay Design Tool (Thermo Fisher Scientific) in order to recognize the mutant (FAM) or the wild-type (VIC) allele. The dPCR was used to analyze tumor cDNA from the carriers; cDNA from sporadic CRC and healthy colon tissue were used as controls.

### Quantitative real-time PCR (qPCR)

For the quantification of the overall gene expression of two *PTPRT* downstream target genes, a qPCR was performed in a 7500 Fast Real-Time PCR System (Applied Biosystems) and using tumor cDNA from the carriers, the TaqMan Gene Expression Master Mix (Applied Biosystems) and specific TaqMan probes designed by Thermo Fisher Scientific (*BCL-XL* assay Hs00236329\_m1 and *SOCS3* assay Hs02330328\_s1). *PSMB4* was used as a housekeeping gene whose levels served as a reference (assay Hs00160598\_m1), and a pool of healthy colon cDNAs was used as a control. All samples were analyzed in triplicates, and the quantification of the relative target gene expression was calculated as  $2^{-\Delta\Delta^{\tau}}$ . The standard deviation was calculated for each sample.

### *PTPRT* mutational screening in an independent series of familial/early-onset non-polyposis CRC cases

Mutational *PTPRT* screening in 473 familial/early-onset MMR-proficient non-polyposis CRC patients was performed using a combination of PCR amplification in pooled DNAs and targeted NGS (Puente et al., 2011). DNA pools were obtained adding equimolecular quantities of each sample (48-96 samples/pool), and used as templates for PCR amplification of each region of interest (i.e. coding exons +/- 20bp) using the Phusion High-Fidelity DNA Polymerase (New England Biolabs. Primers are available upon request. PCR products were purified (QIAquick PCR Purification Kit, Qiagen,), quantified (NanoDrop<sup>TM</sup>, Thermo Fisher Scientific) and mixed in equimolecular quantities. These were ligated and used for paired-end library preparation for subsequent sequencing in a HiSeq 2000 (Illumina) at Centro Nacional de Análisis Genómico (CNAG, Barcelona, Spain). Details of the data analysis are shown in Terradas et al. 2019 (Terradas et al., 2019). Variant-specific KASP genotyping assays (LGC Genomics) and Sanger sequencing were used for validation and identification of the carriers of each variant at STAB VIDA (Caparica, Portugal) and Macrogen (Amsterdam, the Netherlands). Data was analyzed with SeqMan Pro (DNASTAR Lasergene 13).

## Results

### *PTPRT* c.4090dup (D1364Gfs\*24) identified in family cc765

Whole-exome sequencing in two affected members and one cancer-free relative of family cc765 (II:5, II:6 and II:7, Figure 1A) revealed a germline *PTPRT* frameshift mutation that was shared by the affected and absent in the unaffected relative. This family fulfilled the Amsterdam II criteria, with 5 members diagnosed of different cancer types in two successive generations (3 CRCs, 1 endometrial and 1 breast cancer), the earliest age of onset being 28 years old (Figure 1A and Supplementary Table S3). The identified variant was

NM.133170.4: c.4090dup, p.(Asp1364GlyfsTer24), which will be from here on abbreviated as D1364Gfs\*24. This variant is not reported in any of the public databases (gnomAD, ExAc, 1000 Genomes) and affects all of *PTPRT* long protein-coding transcripts, causing the loss of the N-terminal end of the protein.

### Other candidate variants in the family

Other candidate variants in this family included *MAP3K6* NM.004672.5: c.2536C>T, p.(Arg846Cys), *ABTB1* NM.032548.3: c.787G>C, p.(Ala263Pro) and *INVSNC\_000009.12* (INVS\_v004):c.3017-5T>G. However, the *PTPRT* variant was the most relevant among all of them, considering both the gene and the effect of the mutation, reason for which it was selected for further characterization. The segregation of these additional candidate variants is shown in Supplementary Table S4.

### *PTPRT* D1364Gfs\*24 affects the second catalytic domain of the protein

The selected *PTPRT* mutation involves the insertion of a guanine between positions 4090 and 4091 of the cDNA (ENST00000373198) (Figure 1B), causing a shift in the reading frame that is translated as the addition of 23 erroneous amino acids followed by a premature stop codon. This alteration is located at the end of the gene, meaning the loss of the last 97 amino acids of the protein and affecting the second phosphatase domain (also known as D2), which is thought to be responsible for the regulation of the enzyme's activity. Figure 2A shows the different protein domains of *PTPRT*, together with the location of the variant and a schematic visualization of the resulting mutant protein. The effect that the truncation is predicted to have on the 3D structure of *PTPRT*'s cytoplasmatic region (including the 2 catalytic domains) can be observed in Figure 2B, showing a considerable gap caused by the mutation. Finally, Figure 2C was adapted from Lui et al. (Lui et al., 2014) to show the effect of the mutation on the sequence of the D2 domain, pointing out those residues in direct contact with the phospho-tyrosine (in grey) that are lost with this mutation.

### *PTPRT* D1364Gfs\*24 segregation study

The result from the segregation study carried out in other family members is shown in Figure 1A. In addition to the two affected probands originally studied (II:6 and II:7), members II:4 and III:5 also carried the variant, while II:2, II:3 and II:5 showed a wild-type *PTPRT*. Positive members include one with CRC diagnosed at 70 (II:6), one with endometrial cancer diagnosed at 28 (II:7), one with breast cancer diagnosed at 66 (II:4) and a healthy but still young relative (III:5). The negative result was observed in two healthy elderly relatives (II:2 and II:5) and a CRC patient diagnosed at a very late age (II:3, diagnosed at 85).

### Tumor second hit analysis

As far as the LOH is concerned, two FFPE tumor blocks could be studied: the CRC of member II:6 and the breast tumor of member II:4. No significant loss of any of the alleles was observed in the CRC, although a slight reduction of the mutant allele was detected in the breast tumor (Supplementary Figure S5). On the other hand, a promoter methylation assay was used to study the methylation status of *PTPRT* promoter in the available tumors at two different sites previously reported (Laczmanska et al., 2013; Peyser et al., 2016). This assay showed that the CRC tumor DNA of one of the mutation carriers (II:6) was hypermethylated at the two *PTPRT* promoter sites tested, as compared to healthy colon DNA from the same carrier, as well as to a pool of healthy colon samples used as a control (Figure 3A). Although to a lesser extent, the same result was observed when DNA from the breast tumor and healthy breast from member II:4 was studied at the promoter site described by Peyser et al. (Peyser et al., 2016) (Figure 3B). However, no methylation was observed in any of the breast samples at the methylation site reported by Laczmanska et al. (Laczmanska et al., 2013). A pyrosequencing assay targeting *PTPRT* promoter confirmed the hypermethylation observed in the CRC of member II:6 compared to its healthy colon tissue (Figure 3C). Although once again more subtle, the breast cancer also showed an increased methylation compared to the healthy breast tissue of member II:4.

### Tumor *PTPRT* allele-specific expression

A digital PCR was then performed in order to check the allele-specific expression of wild-type and mutant

*PTPRT* in the tumor. This assay showed that there was expression of both alleles (wild type and mutant) in tumor cDNA from a *PTPRT* mutation carrier (II:6). Interestingly, a significant reduction in the expression of the wild-type allele was observed in the CRC compared to the healthy colon from the same individual (Figure 4), while no alteration in the expression of the mutant allele could be appreciated. Unfortunately, no results could be obtained from the breast tumor of member II:4.

### Altered expression of *PTPRT* downstream target genes in the tumors from two carriers

In order to check the downstream consequences of the *PTPRT* mutation, a Taqman real-time qPCR was performed to evaluate the expression of *PTPRT* target genes *BCL2-XL* and *SOCS3* in the tumors developed by family members II:6 and II:4. As shown in Figure 5A, *BCL2-XL* was significantly overexpressed in the colon tumor from member II:6 when compared to a healthy colon cDNA pool. In the same way, the breast tumor from member II:4 showed a consistent higher *BCL2-XL* expression than a healthy breast sample used as a control (Figure 5B). On the other hand, *SOCS3* seemed to be considerably underexpressed in both tumors (CRC from II:6 and breast cancer from II:4), as shown in Figure 5C and D.

### *PTPRT* screening in additional CRC families

The mutational screening of *PTPRT* in 473 additional CRC families revealed another germline missense variant that passed the filtering strategy used for our cohort, NM\_133170.4: c.2837C>G, p.(Ser946Cys) (rs866132388). This variant was found in a Bethesda-positive family and is rare in the general population (MAF=0.00041 according to gnomAD). In addition, it is predicted to be damaging by all 5 *in silico* programs used and affects the first phosphatase domain of the protein (D1).

### Discussion

FCCTX comprises a group of HNPCC families with a higher risk of developing CRC and other associated cancers, but whose genetic basis is still unknown. Some of the genes that have been associated with FCCTX in recent studies include *RPS20* (Nieminen et al., 2014), *BRCA2* (Garre et al., 2015) and other fanconi anemia genes such as *FAN1* or *BRIP1* (Esteban-Jurado et al., 2016; Seguí et al., 2015; Smith et al., 2013), *BMPR1A* (Evans et al., 2018), *SEMA4* (Schulz et al., 2014), *OGG1* (Garre et al., 2011) and *SETD6* (Martín-Morales et al., 2017). However most cases remain unexplained (Valle, 2017; Zetner & Bisgaard, 2017). With the aim of identifying new genes involved in the cancer predisposition of FCCTX, the whole exome was sequenced in 2 or 3 members of 13 FCCTX families. A thorough filtering and prioritization of the identified variants allowed a final selection of candidate variants for each family.

Here we describe the most promising candidate variant for family cc765, a novel frameshift mutation in the *PTPRT* gene: c.4090dup p.(Asp1364GlyfsTer24). *PTPRT* encodes a tyrosine phosphatase that has been proven to behave as a tumor suppressor that is involved in relevant pathways, such as the PI3K-Akt and the IL6-JAK-STAT3 pathway, through which it regulates the expression of genes involved in cell survival, apoptosis, cell proliferation, growth and migration (X. Zhang et al., 2007; Y. Zhao et al., 2017). In fact, *PTPRT* somatic inactivating alterations are frequently found in many tumors, including CRC, and have been reported to act as driver mutations that promote tumor development and progression (L.-E. Wang et al., 2013). Based on the relevance of the gene and the effect of the mutation, this variant was selected for further characterization.

*PTPRT* D1364Gfs\*24 showed a compatible cosegregation with the disease within the family, given that it was carried by 3 members affected with different cancers while it was not present in two elderly cancer-free relatives aged 91 and 85. However, it was also absent in a relative diagnosed with CRC at the age of 85, but taking into account the elevated age of onset in this patient and the prevalence of CRC in the general population this could be perfectly explained as a phenocopy. The cancers of which the *PTPRT* mutation carriers had been diagnosed included two from the HNPCC spectrum (CRC and endometrial cancer) and a breast cancer, which although does not belong to the spectrum occurs with relative frequency within CRC families.

On the other hand, there was not a clear LOH of the wild-type allele in any of the tumors tested. Nonetheless,

*PTPRT* promoter has been recently reported to be frequently hypermethylated in sporadic CRC and other tumors (Laczmanska et al., 2013; Peyser et al., 2016). Indeed, the promoter region of *PTPRT* was found to be hypermethylated in the two tumors of the carriers that were tested (breast and colon tumors), which could be a different mechanism of inactivation of the wild-type allele in the tumors from the carriers. In fact, an allele-specific expression assay showed that the expression of *PTPRT*'s wild-type allele was significantly reduced in the colorectal tumor when compared to healthy colon from the same individual, while no decrease was observed in the expression of the mutant allele. This supports that the epigenetic silencing mainly affects the wild-type allele and could be considered a second hit involved in the inactivation of this tumor suppressor gene.

Regarding the effects of the variant on the protein, D1364Gfs\*24 is a frameshift mutation that affects *PTPRT*'s second catalytic domain, known as D2. *PTPRT* D1364Gfs\*24 results in the loss of the last 97 amino acids of the protein, including 36.2% of the D2 domain and a considerable amount of essential D2 residues. Actually, the majority (69.2%) of residues directly surrounding the substrate's phospho-tyrosine are lost with this mutation (Lui et al., 2014). Although the first phosphatase domain (D1) is the one known to be responsible for the phosphatase activity of the protein *per se*, D2 is responsible for the regulation of this activity and has been proven to be essential for *PTPRT*'s activity (Y. Zhao et al., 2017). As a matter of fact, Wang et al. reported that just a missense mutation affecting D2's residue 1368, which is lost in our mutant, was enough to decrease the enzyme's activity by half (Z. Wang et al., 2004). The relevance of this second catalytic domain was also pointed out by Zhang et al., who showed how the deletion of the D2 domain had significant effects on the levels of phosphorylated *PTPRT* substrates and the expression of its downstream target genes (X. Zhang et al., 2007). Therefore, it can be predicted that this mutation will result in significant consequences for the activity of this phosphatase.

*PTPRT* is known to dephosphorylate two main target proteins, STAT3 and paxillin (X. Zhang et al., 2007; Y. Zhao et al., 2017, 2010), both of which are well-known oncogenes (Bromberg et al., 1999). These two proteins are activated upon phosphorylation by different protein tyrosine kinases, so the *PTPRT*-mediated removal of the phosphate group results in their inactivation. This results, in turn, in the inhibition of their downstream pathways, through a decreased phosphorylation of paxillin's target proteins (Y. Zhao et al., 2017, 2010) and a decreased expression of STAT3's target genes (X. Zhang et al., 2007). *BCL-XL* and *SOCS3* are two of those STAT3's target genes, which have been proven to show increased expression upon *PTPRT* depletion, and even upon deletion of the D2 domain (X. Zhang et al., 2007). Consistent with the hypothesis that this germline *PTPRT* variant may be involved in the cancers of this FCCTX family, the tumors from the two carriers tested presented a significantly increased expression of *BCL-XL*, which is an oncogenic driver in CRC (Scherr et al., 2016). This was observed in both the colon and breast tumors when compared to healthy tissue controls.

In contrast, *SOCS3* expression was decreased in both tumors. Nonetheless, SOCS proteins are negative feedback regulators of the JAK-STAT signaling pathway (Inagaki-Ohara, Kondo, Ito, & Yoshimura, 2013; Jiang et al., 2017), and it has been proven that *SOCS3* is usually downregulated in CRC, even when *IL-6* and *STAT3* are upregulated (Chu et al., 2017). This is thought to occur through different mechanisms, such as the hypermethylation of *SOCS3* gene promoters, allowing inflammatory cytokines IL-6 to activate STAT3's signaling pathway while inhibiting the expression of *SOCS3* (Chu et al., 2017), with the purpose of inactivating its negative feedback. This negative regulation of *SOCS3* expression, mediated by the activation of IL-6/STAT3, leads to imbalance and sustained activation of STAT3 signaling pathway (Chu et al., 2017). The same study by Chu et al. also showed that SOCS3 plays an important role inhibiting tumor development and that reduced *SOCS3*'s expression affects tumorigenesis and CRC progression, promoting growth and metastasis (Chu et al., 2017). For all the things mentioned, both results are compatible with a pathogenic role of this *PTPRT* variant.

As previously discussed, *PTPRT*'s association with cancer has been well studied, but this is the first time that *PTPRT* is linked to hereditary cancer. Interestingly, a somatic mutation affecting the same codon (COSV62009665) is associated with CRC according to COSMIC (Tate et al., 2019). Even though the role

of this protein in tumor development is undeniable, more studies are needed to confirm its involvement as a cancer susceptibility gene. Studying this gene in a larger cohort would help with this task. As a matter of fact, the screening of *PTPRT* in an independent familial/early-onset CRC cohort identified one additional rare missense germline variant located inside the D1 domain in an early-onset CRC patient. However, the functional effect of this variant has not been determined.

Last but not least, it should be pointed out that even though this *PTPRT* mutation had the highest potential for the explanation of the increased cancer risk, another three candidate variants were prioritized for this family: two missense variants in *MAP3K6* and *ABTB1*, and a splice region variant in *INVS*. *MAP3K6* is involved in the regulation of *VEGF* expression and has also been reported to act as a tumor suppressor (Gaston et al., 2014). In addition, germline mutations in this gene have been associated with familial gastric cancer (Gaston et al., 2014). *ABTB1* is a mediator of the PTEN signaling pathway reported to suppress the growth of cancer cells by the inhibition of the cell cycle (Unoki & Nakamura, 2001). Finally, *INVS* acts as a molecular switch between the different Wnt signaling pathways, inhibiting the canonical Wnt pathway (Simons et al., 2005), and homozygous *INVS* mutations have been associated with juvenile nephronophthisis (Bellavia et al., 2010). Although *PTPRT*D1364Gfs\*24 is the best candidate variant for this family and the results presented in this report support its causality, we cannot rule out the possibility that these candidate variants – or even other genetic or environmental factors – may be contributing, independently or together, to the increased cancer susceptibility of the family or modifying the effect of this *PTPRT* mutation.

Taken together, the results here presented point to a probable causal role of the germline variant *PTPRT* c.4090dup p.(Asp1364GlyfsTer24) in the cancer susceptibility of the carrier family. For that reason, we propose *PTPRT* as a novel cancer predisposition gene. However, more research is necessary to confirm the causality, penetrance, conferred risk and preferred cancer location. The screening of this gene in additional familial colorectal cancer cohorts – or even in other high-risk families – will help us clarify its role in cancer predisposition. Although *PTPRT*'s role in cancer initiation and progression has been well established, this is the first time that a *PTPRT* germline variant is linked with cancer susceptibility and hereditary cancer, which highlights the relevance of this work.

## Acknowledgements

This work was supported by grants PI-16/01292 and PI-19/1366 from the Carlos III Health Institute (Spain) and the European Regional Development Funds. A short stay of LMM at Dr. Zhenghe Wang's lab, in Case Western Reserve University (Cleveland, USA), was supported by a travel fellowship of the European Association for Cancer Research. The authors would like to thank the families for taking part in the study. We would also like to acknowledge Dr. Zhenghe Wang for his collaboration, Paula Diaque, Isabel Diaz Millan and Durgadevi Ravillah for their technical assistance, and the Biobank of Hospital Clinico San Carlos (Madrid, Spain) for the FFPE blocks, sections and pathology records.

## Conflict of interest statement

The authors declare no conflicts of interests.

## Data availability statement

The datasets generated and analyzed during the current study are available from the corresponding author upon reasonable request.

## Web resources

Condel ([bbglab.irbbarcelona.org/fannsd/](http://bbglab.irbbarcelona.org/fannsd/)); COSMIC ([cancer.sanger.ac.uk](http://cancer.sanger.ac.uk)); Ensembl ([www.ensembl.org](http://www.ensembl.org)); Genecards ([www.genecards.org](http://www.genecards.org)); HSF ([www.umd.be/HSF/](http://www.umd.be/HSF/)); Mutation Mapper ([www.cbiportal.org/mutation\\_mapper](http://www.cbiportal.org/mutation_mapper)); MutationTaster ([www.mutationtaster.org](http://www.mutationtaster.org)); OMIM ([www.omim.org](http://www.omim.org)); Pathcards ([pathcards.genecards.org](http://pathcards.genecards.org)); PolyPhen 2 ([genetics.bwh.harvard.edu/pph2/](http://genetics.bwh.harvard.edu/pph2/)); Primer 3 ([primer3.ut.ee](http://primer3.ut.ee)); PROVEAN ([provean.jcvi.org/](http://provean.jcvi.org/)); Reactome ([reactome.org](http://reactome.org)); SIFT ([sift.bii.a](http://sift.bii.a)

star.edu.sg); SMART ([smart.embl-heidelberg.de](http://smart.embl-heidelberg.de)); STRING ([string-db.org](http://string-db.org)); SWISS-MODEL ([swissmodel.expasy.org](http://swissmodel.expasy.org)); UniProt ([www.uniprot.org](http://www.uniprot.org)).

## References

- Belhadj, S., Quintana, I., Mur, P., Munoz-Torres, P. M., Alonso, M. H., Navarro, M., ... Valle, L. (2019). NTHL1 biallelic mutations seldom cause colorectal cancer, serrated polyposis or a multi-tumor phenotype, in absence of colorectal adenomas. *Scientific Reports* , *9* (1), 9020. <https://doi.org/10.1038/s41598-019-45281-1>
- Bellavia, S., Dahan, K., Terryn, S., Cosyns, J.-P., Devuyt, O., & Pirson, Y. (2010). A homozygous mutation in INVS causing juvenile nephronophthisis with abnormal reactivity of the Wnt/beta-catenin pathway. *Nephrology, Dialysis, Transplantation: Official Publication of the European Dialysis and Transplant Association - European Renal Association* , *25* (12), 4097–4102. <https://doi.org/10.1093/ndt/gfq519>
- Besco, J. A., Hooft van Huijsdijnen, R., Frosthalm, A., & Rotter, A. (2006). Intracellular substrates of brain-enriched receptor protein tyrosine phosphatase rho (RPTPrho/PTPRT). *Brain Research* , *1116* (1), 50–57. <https://doi.org/10.1016/j.brainres.2006.07.122>
- Bromberg, J. F., Wrzeszczynska, M. H., Devgan, G., Zhao, Y., Pestell, R. G., Albanese, C., & Darnell, J. E. (1999). Stat3 as an oncogene. *Cell* , *98* (3), 295–303.
- Chu, Q., Shen, D., He, L., Wang, H., Liu, C., & Zhang, W. (2017). Prognostic significance of SOCS3 and its biological function in colorectal cancer. *Gene* , *627* , 114–122. <https://doi.org/10.1016/j.gene.2017.06.013>
- Darnell, J. E. (2005). Validating Stat3 in cancer therapy. *Nature Medicine* , *11* (6), 595–596. <https://doi.org/10.1038/nm0605-595>
- Esteban-Jurado, C., Franch-Expósito, S., Muñoz, J., Ocaña, T., Carballal, S., López-Cerón, M., ... Castellví-Bel, S. (2016). The Fanconi anemia DNA damage repair pathway in the spotlight for germline predisposition to colorectal cancer. *European Journal of Human Genetics: EJHG* , *24* (10), 1501–1505. <https://doi.org/10.1038/ejhg.2016.44>
- Evans, D. R., Green, J. S., & Woods, M. O. (2018). Screening of BMPR1a for pathogenic mutations in familial colorectal cancer type X families from Newfoundland. *Familial Cancer* , *17* (2), 205–208. <https://doi.org/10.1007/s10689-017-0016-8>
- Garre, P., Briceno, V., Xicola, R. M., Doyle, B. J., de la Hoya, M., Sanz, J., ... Caldes, T. (2011). Analysis of the Oxidative Damage Repair Genes NUDT1, OGG1, and MUTYH in Patients from Mismatch Repair Proficient HNPCC Families (MSS-HNPCC). *Clinical Cancer Research* , *17* (7), 1701–1712. <https://doi.org/10.1158/1078-0432.CCR-10-2491>
- Garre, P., Martín, L., Sanz, J., Romero, A., Tosar, A., Bando, I., ... Caldés, T. (2015). BRCA2 gene: A candidate for clinical testing in familial colorectal cancer type X. *Clinical Genetics* , *87* (6), 582–587. <https://doi.org/10.1111/cge.12427>
- Gaston, D., Hansford, S., Oliveira, C., Nightingale, M., Pinheiro, H., Macgillivray, C., ... Bedard, K. (2014). Germline mutations in MAP3K6 are associated with familial gastric cancer. *PLoS Genetics* , *10* (10), e1004669. <https://doi.org/10.1371/journal.pgen.1004669>
- Hunter, T. (2009). Tyrosine phosphorylation: Thirty years and counting. *Current Opinion in Cell Biology* , *21* (2), 140–146. <https://doi.org/10.1016/j.ceb.2009.01.028>
- Inagaki-Ohara, K., Kondo, T., Ito, M., & Yoshimura, A. (2013). SOCS, inflammation, and cancer. *JAK-STAT* , *2* (3), e24053. <https://doi.org/10.4161/jkst.24053>
- Jiang, M., Zhang, W., Liu, P., Yu, W., Liu, T., & Yu, J. (2017). Dysregulation of SOCS-Mediated Negative Feedback of Cytokine Signaling in Carcinogenesis and Its Significance in Cancer Treatment. *Frontiers in Immunology* , *8* . <https://doi.org/10.3389/fimmu.2017.00070>

- Julien, S. G., Dubé, N., Hardy, S., & Tremblay, M. L. (2011). Inside the human cancer tyrosine phosphatome. *Nature Reviews. Cancer* ,11 (1), 35–49. <https://doi.org/10.1038/nrc2980>
- Laczmanska, I., Karpinski, P., Bebenek, M., Sedziak, T., Ramsey, D., Szmida, E., & Sasiadek, M. M. (2013). Protein tyrosine phosphatase receptor-like genes are frequently hypermethylated in sporadic colorectal cancer. *Journal of Human Genetics* , 58 (1), 11–15. <https://doi.org/10.1038/jhg.2012.119>
- Lindor, N. M. (2009). Familial colorectal cancer type X: The other half of hereditary nonpolyposis colon cancer syndrome. *Surgical Oncology Clinics of North America* , 18 (4), 637–645. <https://doi.org/10.1016/j.soc.2009.07.003>
- Lui, V. W. Y., Peyser, N. D., Ng, P. K.-S., Hritz, J., Zeng, Y., Lu, Y., ... Grandis, J. R. (2014). Frequent mutation of receptor protein tyrosine phosphatases provides a mechanism for STAT3 hyperactivation in head and neck cancer. *Proceedings of the National Academy of Sciences of the United States of America* , 111 (3), 1114–1119. <https://doi.org/10.1073/pnas.1319551111>
- Martín-Morales, L., Feldman, M., Vershinin, Z., Garre, P., Caldés, T., & Levy, D. (2017). SETD6 dominant negative mutation in familial colorectal cancer type X. *Human Molecular Genetics* ,26 (22), 4481–4493. <https://doi.org/10.1093/hmg/ddx336>
- Nieminen, T. T., O’Donohue, M.-F., Wu, Y., Lohi, H., Scherer, S. W., Paterson, A. D., ... Peltomäki, P. (2014). Germline Mutation of RPS20, Encoding a Ribosomal Protein, Causes Predisposition to Hereditary Nonpolyposis Colorectal Carcinoma Without DNA Mismatch Repair Deficiency. *Gastroenterology* , 147 (3), 595-598.e5. <https://doi.org/10.1053/j.gastro.2014.06.009>
- Peyser, N. D., Freilino, M., Wang, L., Zeng, Y., Li, H., Johnson, D. E., & Grandis, J. R. (2016). Frequent promoter hypermethylation of PTPRT increases STAT3 activation and sensitivity to STAT3 inhibition in head and neck cancer. *Oncogene* , 35 (9), 1163–1169. <https://doi.org/10.1038/onc.2015.171>
- Puente, X. S., Pinyol, M., Quesada, V., Conde, L., Ordóñez, G. R., Villamor, N., ... Campo, E. (2011). Whole-genome sequencing identifies recurrent mutations in chronic lymphocytic leukaemia. *Nature* , 475 (7354), 101–105. <https://doi.org/10.1038/nature10113>
- Scherr, A.-L., Gdynia, G., Salou, M., Radhakrishnan, P., Duglova, K., Heller, A., ... Koehler, B. C. (2016). Bcl-xL is an oncogenic driver in colorectal cancer. *Cell Death & Disease* , 7 (8), e2342–e2342. <https://doi.org/10.1038/cddis.2016.233>
- Schulz, E., Klampfl, P., Holzapfel, S., Janecke, A. R., Ulz, P., Renner, W., ... Sill, H. (2014). Germline variants in the SEMA4A gene predispose to familial colorectal cancer type X. *Nature Communications* , 5 , 5191. <https://doi.org/10.1038/ncomms6191>
- Seguí, N., Mina, L. B., Lázaro, C., Sanz-Pamplona, R., Pons, T., Navarro, M., ... Valle, L. (2015). Germline Mutations in FAN1 Cause Hereditary Colorectal Cancer by Impairing DNA Repair. *Gastroenterology* , 149 (3), 563–566. <https://doi.org/10.1053/j.gastro.2015.05.056>
- Simons, M., Gloy, J., Ganner, A., Bullerkotte, A., Bashkurov, M., Krönig, C., ... Walz, G. (2005). Inversin, the gene product mutated in nephronophthisis type II, functions as a molecular switch between Wnt signaling pathways. *Nature Genetics* , 37 (5), 537–543. <https://doi.org/10.1038/ng1552>
- Singh, V., Ram, M., Kumar, R., Prasad, R., Roy, B. K., & Singh, K. K. (2017). Phosphorylation: Implications in Cancer. *The Protein Journal* , 36 (1), 1–6. <https://doi.org/10.1007/s10930-017-9696-z>
- Smith, C. G., Naven, M., Harris, R., Colley, J., West, H., Li, N., ... Cheadle, J. P. (2013). Exome Resequencing Identifies Potential Tumor-Suppressor Genes that Predispose to Colorectal Cancer. *Human Mutation* , 34 (7), 1026–1034. <https://doi.org/10.1002/humu.22333>
- Tate, J. G., Bamford, S., Jubb, H. C., Sondka, Z., Beare, D. M., Bindal, N., ... Forbes, S. A. (2019). COSMIC: The Catalogue Of Somatic Mutations In Cancer. *Nucleic Acids Research* , 47 (D1), D941–D947.

<https://doi.org/10.1093/nar/gky1015>

Terradas, M., Munoz-Torres, P. M., Belhadj, S., Aiza, G., Navarro, M., Brunet, J., ... Valle, L. (2019). Contribution to colonic polyposis of recently proposed predisposing genes and assessment of the prevalence of NTHL1- and MSH3-associated polyposes. *Human Mutation* . <https://doi.org/10.1002/humu.23853>

Tonks, N. K. (2006). Protein tyrosine phosphatases: From genes, to function, to disease. *Nature Reviews. Molecular Cell Biology* , 7 (11), 833–846. <https://doi.org/10.1038/nrm2039>

Umar, A., Boland, C. R., Terdiman, J. P., Syngal, S., de la Chapelle, A., Rüschoff, J., ... Srivastava, S. (2004). Revised Bethesda Guidelines for hereditary nonpolyposis colorectal cancer (Lynch syndrome) and microsatellite instability. *Journal of the National Cancer Institute* , 96 (4), 261–268.

Unoki, M., & Nakamura, Y. (2001). Growth-suppressive effects of BPOZ and EGR2, two genes involved in the PTEN signaling pathway. *Oncogene* , 20 (33), 4457–4465. <https://doi.org/10.1038/sj.onc.1204608>

Valle, L. (2017). Recent Discoveries in the Genetics of Familial Colorectal Cancer and Polyposis. *Clinical Gastroenterology and Hepatology* , 15 (6), 809–819. <https://doi.org/10.1016/j.cgh.2016.09.148>

Vasen, H. F., Mecklin, J. P., Khan, P. M., & Lynch, H. T. (1991). The International Collaborative Group on Hereditary Non-Polyposis Colorectal Cancer (ICG-HNPCC). *Diseases of the Colon and Rectum* , 34 (5), 424–425.

Vasen, H. F., Watson, P., Mecklin, J. P., & Lynch, H. T. (1999). New clinical criteria for hereditary nonpolyposis colorectal cancer (HNPCC, Lynch syndrome) proposed by the International Collaborative group on HNPCC. *Gastroenterology* , 116 (6), 1453–1456.

Wang, L.-E., Gorlova, O. Y., Ying, J., Qiao, Y., Weng, S.-F., Lee, A. T., ... Wei, Q. (2013). Genome-wide association study reveals novel genetic determinants of DNA repair capacity in lung cancer. *Cancer Research* , 73 (1), 256–264. <https://doi.org/10.1158/0008-5472.CAN-12-1915>

Wang, Z., Shen, D., Parsons, D. W., Bardelli, A., Sager, J., Szabo, S., ... Velculescu, V. E. (2004). Mutational analysis of the tyrosine phosphatome in colorectal cancers. *Science (New York, N. Y.)* , 304 (5674), 1164–1166. <https://doi.org/10.1126/science.1096096>

Zetner, D. B., & Bisgaard, M. L. (2017). Familial Colorectal Cancer Type X. *Current Genomics* , 18 (4). <https://doi.org/10.2174/1389202918666170307161643>

Zhang, P., Zhao, Y., Zhu, X., Sedwick, D., Zhang, X., & Wang, Z. (2011). Cross-talk between phospho-STAT3 and PLC $\gamma$ 1 plays a critical role in colorectal tumorigenesis. *Molecular Cancer Research: MCR* , 9 (10), 1418–1428. <https://doi.org/10.1158/1541-7786.MCR-11-0147>

Zhang, X., Guo, A., Yu, J., Possemato, A., Chen, Y., Zheng, W., ... Wang, Z. J. (2007). Identification of STAT3 as a substrate of receptor protein tyrosine phosphatase T. *Proceedings of the National Academy of Sciences of the United States of America* , 104 (10), 4060–4064. <https://doi.org/10.1073/pnas.0611665104>

Zhao, S., Sedwick, D., & Wang, Z. (2015). Genetic alterations of protein tyrosine phosphatases in human cancers. *Oncogene* , 34 (30), 3885–3894. <https://doi.org/10.1038/onc.2014.326>

Zhao, Y., Scott, A., Zhang, P., Hao, Y., Feng, X., Somasundaram, S., ... Wang, Z. (2017). Regulation of paxillin-p130-PI3K-AKT signaling axis by Src and PTPRT impacts colon tumorigenesis. *Oncotarget* , 8 (30), 48782–48793. <https://doi.org/10.18632/oncotarget.10654>

Zhao, Y., Zhang, X., Guda, K., Lawrence, E., Sun, Q., Watanabe, T., ... Wang, Z. (2010). Identification and functional characterization of paxillin as a target of protein tyrosine phosphatase receptor T. *Proceedings of the National Academy of Sciences of the United States of America* , 107 (6), 2592–2597. <https://doi.org/10.1073/pnas.0914884107>

## Figure legends

**Figure 1. Pedigree of the family carrying *PTPRT*D1364Gfs\*24.**

(A) Pedigree of Amsterdam II family cc765, where *PTPRT* c.4090dup p.(Asp1364GlyfsTer24), was identified. Whole-exome sequencing was done in family members II:5, II:6 and II:7 (in a grey box), and the cosegregation analyzed in II:2, II:3, II:4 and III:5. Four individuals were carriers (+), while three were non-carriers (WT). Cancer-affected members are marked with a black corner; bottom right: CRC, top right: endometrial cancer (EC), bottom left: breast cancer (BC). The age at diagnosis or current age of healthy members is included beneath each individual (in years). B) Electropherogram of the wild-type and mutant sequence of the *PTPRT* gene. The arrows show the point where the guanine is inserted.

**Figure 2. Effect of *PTPRT* D1364Gfs\*24 on the protein structure.**

(A) Schematic representation of *PTPRT* protein domains, with the location of the studied mutation and the resulting mutant protein (below). B) 3D representation of the cytoplasmatic region of wild-type (left) and mutant (right) *PTPRT*, showing the effect of the truncation. 3D models were obtained by SWISS-MODEL. C) Amino acid sequence of *PTPRT*'s D2 domain with the effect produced by the mutation. Those residues directly surrounding the pTyr are marked in grey. Underlined are all the residues that differ between the two forms of *PTPRT*. Modified from Lui et al. 2013.

**Figure 3. *PTPRT* promoter is hypermethylated in the colon and breast cancers of two mutation carriers.**

(A+B) *PTPRT* promoter methylation obtained by MSP of two different promoter sites previously described. Panel A shows the methylation status of the CRC vs healthy colon tissue of member II:6 and a healthy colon pool. Panel B shows the methylation status of the breast cancer vs healthy breast of member II:4 and a commercial healthy breast sample. (C) *PTPRT* promoter methylation status (%) obtained by pyrosequencing for the same samples analyzed in A, together with methylated and unmethylated commercial controls.

**Figure 4. Allele-specific expression of wild-type and D1364Gfs\*24 *PTPRT*.**

(A) Digital PCR visualization of the allele-specific expression assay performed in the healthy colon tissue (top) and colorectal cancer (CRC) (bottom) of cc765 family member II:6. The FAM dye detects the mutant allele (circled with dashed line), while the VIC dye detects the wild-type allele (circled with solid line). B) Quantification of the allele-specific expression obtained by digital PCR presented as Target/Total, where "Target" is the mutant *PTPRT* allele. Data was collected from two independent experiments, and the error bars correspond to the confidence intervals.

**Figure 5. Expression of *STAT3* target genes in the tumors of two *PTPRT* mutation carriers.**

Quantification of *BCL-XL* (A+B) and *SOCS3* (C+D) expression obtained by qPCR in the tumors of cc765 family members II:6 (A+C) and II:4 (B+D), affected with colorectal and breast cancer, respectively. Data was collected from three technical replicates and represent 2 independent experiments; the error bars represent the standard deviation.

**Appendix: ORCID IDs of co-authors**

Lorena Martín-Morales 0000-0002-1970-8872

Victor Lorca 0000-0002-3681-4319

Pedro Pérez-Segura 0000-0001-5049-7199

Patricia Llovet 0000-0003-0190-2105

Vanesa García-Barberán 0000-0002-2531-0203

María Luisa González-Morales

Sami Belhad

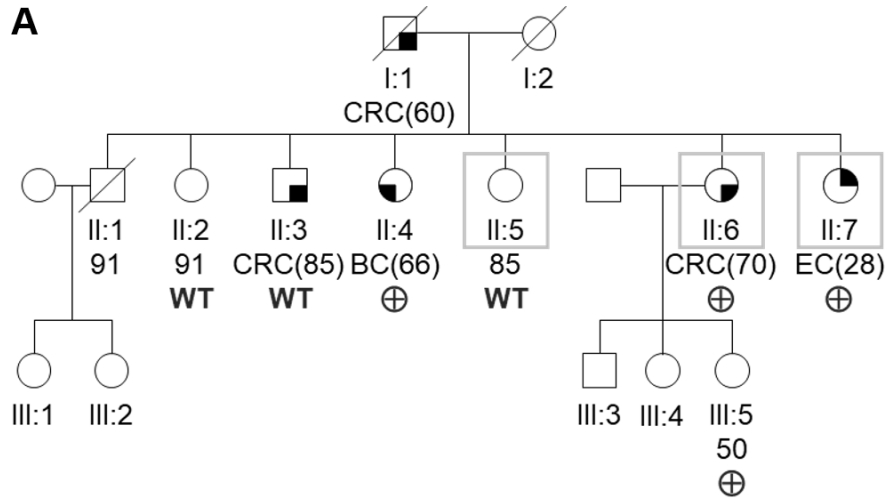
Gabriel Capellá 0000-0002-2159-1351

Laura Valle 0000-0003-0371-0844

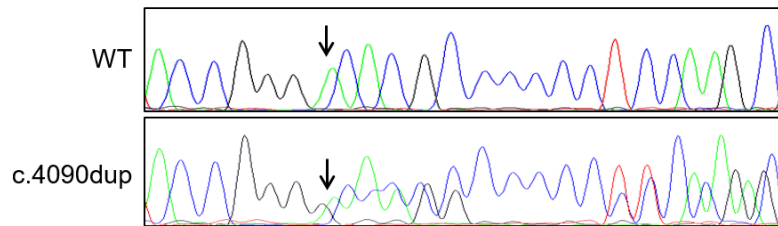
Miguel de la Hoya 0000-0002-8113-1410

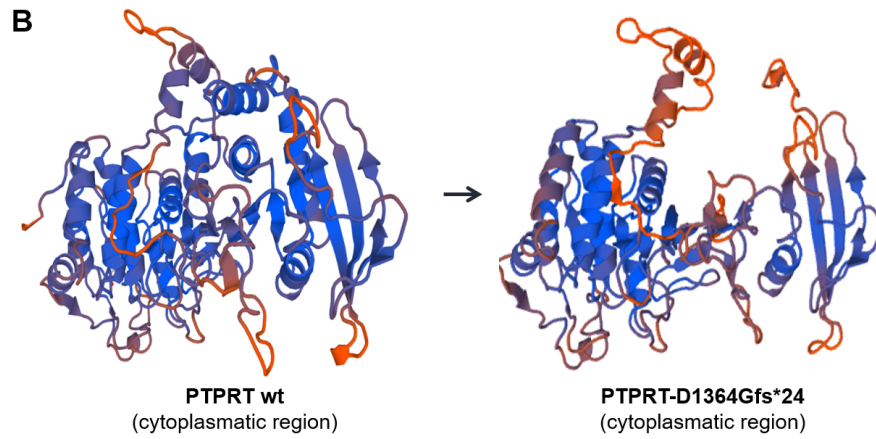
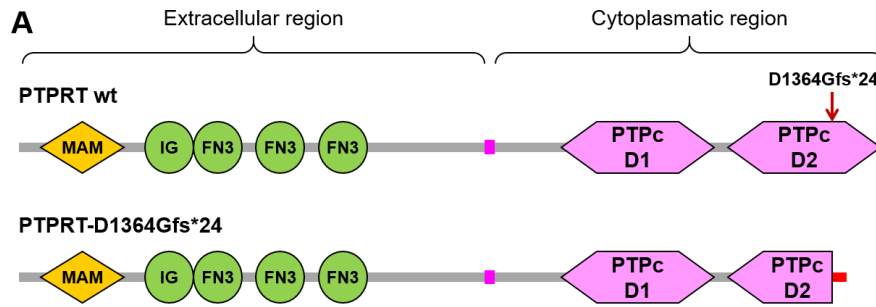
Pilar Garre 0000-0001-8285-4138

Trinidad Caldés 0000-0002-1038-5392



**B** *PTPRT* (ENST00000373198), NM\_133170:c.4090dup



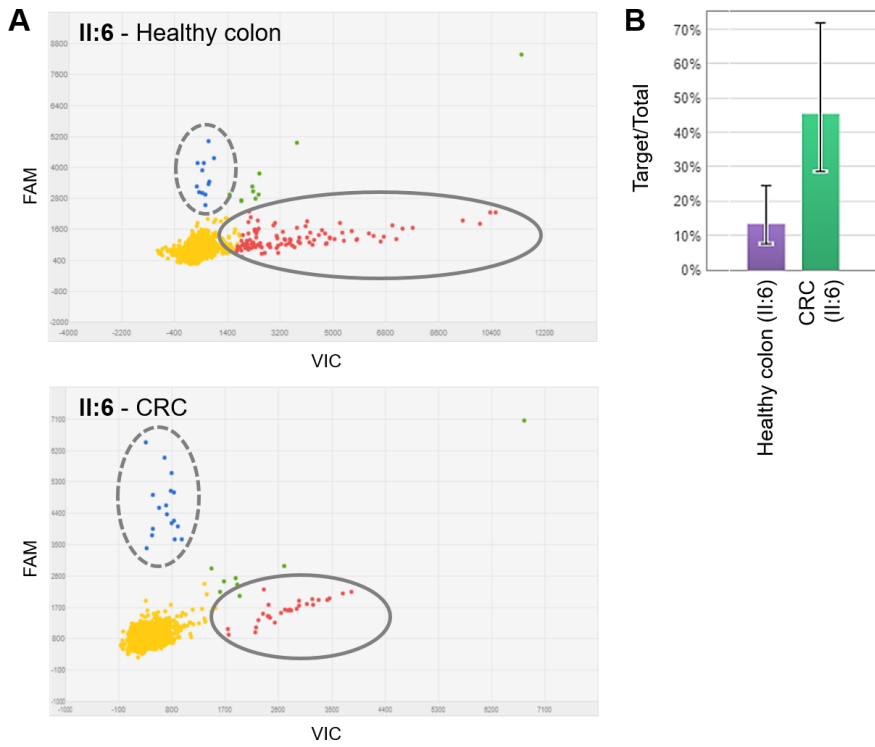
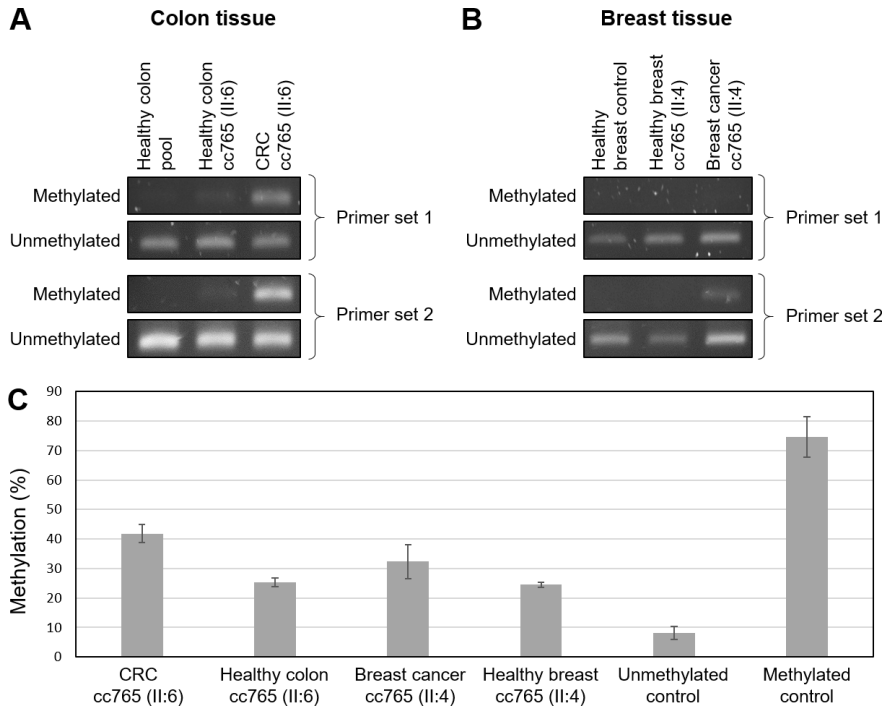


**C D2 sequence**

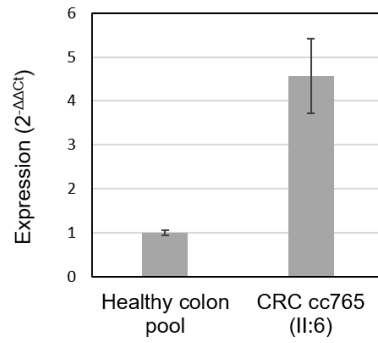
QIKDEFQTLNIVTPRVRPEDCSIGLLPRNHDKNR  
**S**MDVLPDRCLPFLISVDGESSNYINAALMDSHK  
 QPAAFVVTQHPLPNTVADFWRVLFDYNCSSVV  
 MLNEMDTAQFCMQYWPEKTSGCYGPQVEFVS  
 ADIDEDIIHRIFRICNMARPQDGYRIVQHLQYIG**W**  
 PAY**R**DTPPSKRSLKVVRRLEKWQEYDGREG  
 RTVVH**CLNGGGRS**GTFC AICSVCEMIQQQNIID  
 VFHIVKTLRNNKSNMV**ET**LEQYKFVYEVALEYLS  
 SF



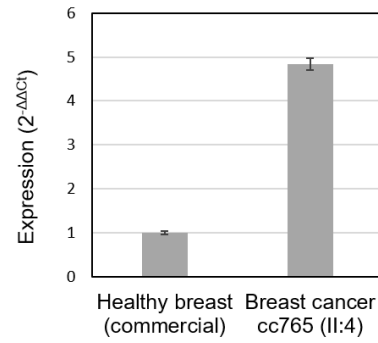
QIKDEFQTLNIVTPRVRPEDCSIGLLPRNHDKNR  
**S**MDVLPDRCLPFLISVDGESSNYINAALMDSHK  
 QPAAFVVTQHPLPNTVADFWRVLFDYNCSSVV  
 MLNEMDTAQFCMQYWPEKTSGCYGPQVEFVS  
 ADIDEDIIHRIFRICNMARPQDGYRIVQHLQYIG**W**  
 PAY**R**GHA**PL**QALSAQSGPTTGEVAGAV



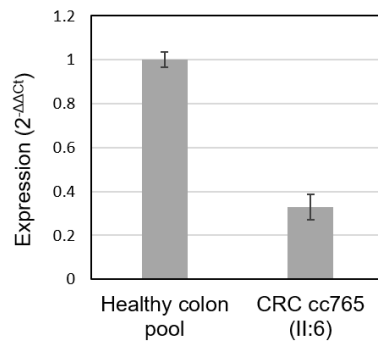
**A** Colon tissue - *BCL-XL*



**B** Breast tissue - *BCL-XL*



**C** Colon tissue - *SOCS3*



**D** Breast tissue - *SOCS3*

